European Journal of Medicinal Chemistry 157 (2018) 1202–1213

Contents lists available at ScienceDirect

European Journal of Medicinal Chemistry

journal homepage: http://www.elsevier.com/locate/ejmech

Research paper

Breathing new life into West Nile virus therapeutics; discovery and study of zafirlukast as an NS2B-NS3 protease inhibitor

Anastasia A. Martinez, Bianca A. Espinosa, Rebecca N. Adamek, Brent A. Thomas, Jennifer Chau, Edwardo Gonzalez, Niroshika Keppetipola, Nicholas T. Salzameda*

Department of Chemistry & Biochemistry, California State University, Fullerton, 800 N. State College, Fullerton, CA, 92831, USA

ARTICLE INFO

Article history:
Received 3 May 2018
Received in revised form
6 August 2018
Accepted 27 August 2018
Available online 31 August 2018

Keywords:
West nile virus
NS2B-NS3 protease
Zafirlukast
Allosteric inhibitor
Serine protease

ABSTRACT

The West Nile virus (WNV) has spread throughout the world causing neuroinvasive diseases with no treatments available. The viral NS2B-NS3 protease is essential for WNV survival and replication in host cells and is a promising drug target. Through an enzymatic screen of the National Institute of Health clinical compound library, we report the discovery of zafirlukast, an FDA approved treatment for asthma, as an inhibitor for the WNV NS2B-NS3 protease. Zafirlukast was determined to inhibit the protease through a mixed mode mechanism with an IC_{50} value of 32 μM. A structure activity relationship study of zafirlukast revealed the cyclopentyl carbamate and *N*-aryl sulfonamide as structural elements crucial for NS2B-NS3 protease inhibition. Replacing the cyclopentyl with a phenyl improved inhibition, resulting in an IC_{50} of 22 μM. Experimental and computational docking analysis support the inhibition model of zafirlukast and analogs binding at an allosteric site on the NS3 protein, thereby disrupting the NS2B cofactor from binding, resulting in protease inhibition.

1. Introduction

The West Nile virus (WNV) is a species of the Flaviviridae family and has been a global epidemic since the 1990's. The virus' mode of transmission is between birds and mosquitoes with humans as accidental hosts via mosquito blood meals [1]. Most cases of WNV infections are asymptomatic, but 20% of infections can manifest into mild symptoms of fever and headaches [2,3]. In serious cases, infections progress into neurological diseases, such as meningitis and encephalitis that can be fatal [2,3]. There is currently no treatment or cure for WNV infections.

The WNV is an enveloped single-stranded, positive-sense RNA virus. The 11 kb genome is transcribed into a single viral polyprotein that contains three structural and seven nonstructural proteins required for WNV replication from host cell to host cell [1]. The structural proteins are the envelope, capsid, and premembrane, while the nonstructural (NS) proteins are designated NS1 to NS5 [4,5]. The viral polyprotein is processed by host cell furin and the WNV NS2B-NS3 protease into the individual structural and nonstructural proteins needed for viral replication in the endoplasmic reticulum (ER) [6].

From a therapeutic standpoint, the NS3 protein is of interest due to its required functions for WNV infection and proliferation. The NS3 protein can function as a 5′-triphosphatase, nucleoside triphosphatase, RNA helicase, and serine protease, which are all important for viral replication [1]. The serine protease activity of the NS3 protein requires the NS2B protein as a cofactor [7]. The NS2B protein has three hydrophobic and one hydrophilic domain [8]. The hydrophobic domains are integrated into the ER membrane, while the hydrophilic domain non-covalently binds to the NS3 protein to form the active serine protease complex [1,8]. The WNV NS2B-NS3 protease active site has the typical serine protease catalytic triad comprised of His51, Asp75, and Ser135 near the *N*-terminus of the NS3 protein [9,10]. The WNV NS2B-NS3 protease is known to cleave the viral polyprotein at basic residues, notably arginine and lysine [10].

The NS2B-NS3 protease is a thoroughly studied target for pharmaceutical treatment of WNV infections, due to the essential role of the protease in viral replication [11]. It has been shown that mutating the NS3 protease into an inactive enzyme is deleterious for further WNV infection [12]. Small molecules featuring a variety of scaffolds [13–15], along with peptides [16–21] have been investigated as WNV NS2B-NS3 protease inhibitors.

The National Institute of Health clinical compound library was

* Corresponding author.
E-mail address: nsalzameda@fullerton.edu (N.T. Salzameda).

https://doi.org/10.1016/j.ejmech.2018.08.077
0223-5234/

screened in search of NS2B-NS3 protease inhibitors. The library screen identified Zafirlukast (Fig. 1) as a promising candidate for NS2B-NS3 protease inhibition.

Zafirlukast, commonly known as Accolate, is an FDA approved orally administered drug for the effective inhibition of smooth muscle airway inflammation for the treatment of asthma [22]. It has also been reported to have antibacterial activity against two oral infections, *Porphyromonas* gingivalis and *Streptococcus* mutants [23]. Zafirlukast contains both a toluic acid-*N*-aryl sulfonamide and cyclopentyl carbamate domains linked via an indole. The large molecular size of zafirlukast provided an ideal starting point for structure activity relationship (SAR) studies to probe WNV NS2B-NS3 protease inhibitor activity. Here, we report the inhibitor kinetic study of zafirlukast and the initial SAR study for NS2B-NS3 protease inhibition. In addition, computational docking analysis identified a possible binding site for zafirlukast on the NS3 protein.

2. Results and discussion

2.1. Inhibitor validation and enzyme inhibitor kinetic study

The NS2B-NS3 protease activity was measured by a fluorescence resonance energy transfer (FRET) enzymatic assay. The assay involves a synthetic reporter peptide that contains both fluorophore and quencher molecules attached to amino acids located across the peptide cleavage site [24]. As the WNV NS2B-NS3 protease cleaves the synthetic peptide an increase in fluorescence from the fluorophore is measured and is proportional to enzymatic activity [24]. The assay was used to identify the inhibitor, validate inhibition, determine the IC_{50} (inhibitor concentration that lowers enzymatic activity by 50%) value and mode of inhibition. The IC_{50} value of zafirlukast was determined to be 32 μM for the NS2B-NS3 protease. Zafirlukast was validated by monitoring inhibition in the presence of detergents at various concentrations. The inhibitor activity of zarfirlukast was consistent with a range of concentrations (0–0.2%) in both CHAPS and Brij35 detergents (Fig. 2). This experiment confirms that the observed inhibitory effects of zafirlukast were specific to the NS2B-NS3 protease and not caused by non-specific aggregation.

In addition, an enzyme inhibitor kinetic study was performed varying both the inhibitor and substrate concentrations to generate a Lineweaver-burke plot (Fig. 3). Based on the plot, zafirlukast inhibits the protease through a mixed inhibition mechanism. This mechanism is further supported by a Michaelis-Menten plot (see supplementary data) at various inhibitor concentrations, which indicates a decrease in the appV_{max} and increase in the appK_m of the enzymatic reaction as the concentration of zafirlukast is increased. This type of mechanism would indicate that zafirlukast is inhibiting the protease by binding at an allosteric site on the protease. This is consistent with previously reported small molecule inhibitors that act via uncompetitive or mixed inhibition modes [13,25,26]. Collectively, these results suggest that inhibitors including zafirlukast bind to an allosteric site on the NS3 protein and either alters the conformation of the NS3 active site or disrupts binding of the cofactor NS2B, to render the NS2B-NS3 protease catalytically inactive.

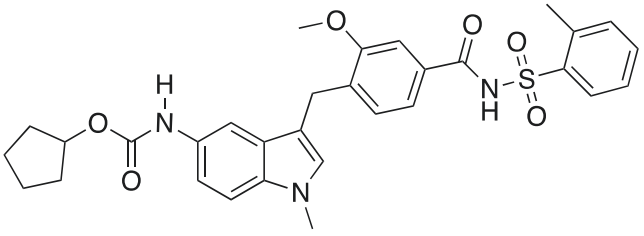

Fig. 1. Zafirlukast is a WNV NS2B-NS3 protease inhibitor.

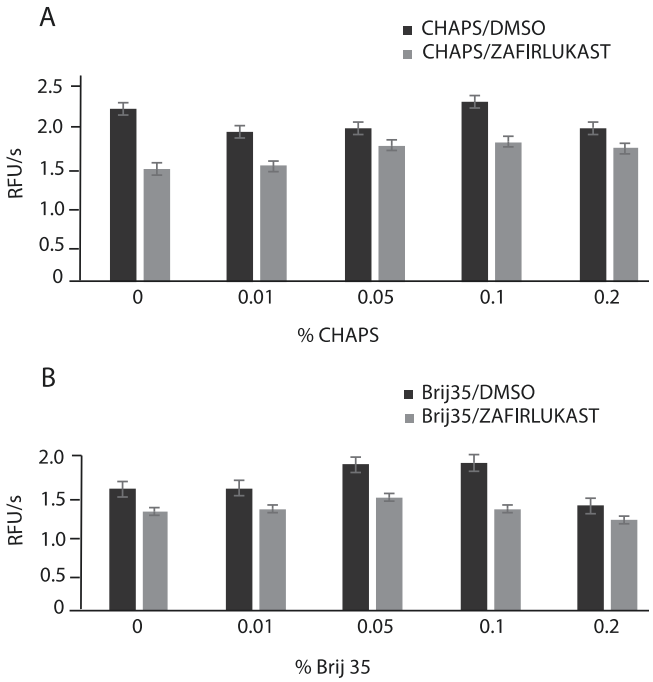

Fig. 2. Zafirlukast inhibition of NS2B-NS3 activity in the presence of various concentrations of CHAPS and Brij35 detergents. The inhibitor activity was consistent in the presence of detergents at varying concentrations.

2.2. Structure activity relationship study

The binding of zafirlukast to the NS2B-NS3 protease was studied through a structure activity relationship (SAR) study via chemical synthesis and enzymatic assays of the analogs. Zafirlukast analogs were synthesized following literature procedures [27,28] and all compounds were examined at 60 μM by the FRET based enzymatic assay to determine the percent of NS2B-NS3 protease inhibition (Table 1) [24]. Zafirlukast contains a toluic acid-*N*-aryl sulfonamide domain connected at the C-2 of the indole. Complete removal of the *N*-aryl sulfonamide (**1**) significantly decreased inhibition. In addition, substituting the sulfonamide for an amide linker (**2**) resulted in similar poor inhibition. These results indicate both the aromatic ring and the sulfonamide group are essential for inhibition. However, the methyl group attached to the benzene of the *N*-aryl sulfonamide was shown to have no significant effects on inhibitor activity, as an analog without the methyl group (**3**) displayed comparable inhibition to zafirlukast. The sulfonamide can aid in binding through hydrogen bonding and orientating groups in a favorable position that cannot be achieved with the amide. It is not clear if the hydrogen bonding or directing ability of the sulfonamide is the element responsible for inhibition.

The toluic acid contains a methoxy group at the meta position. Removal of the methoxy (**4**) lowers inhibitor activity, but not greatly. This would indicate that either the methoxy is not in close hydrogen bond distance to residues of the protein or the methoxy is donating electron density to the aromatic ring, thereby increasing the strength of π-stacking interactions between the phenyl and nearby aromatic residues. Removal of the methoxy group would not result in complete loss of the phenyl-residue interaction, but

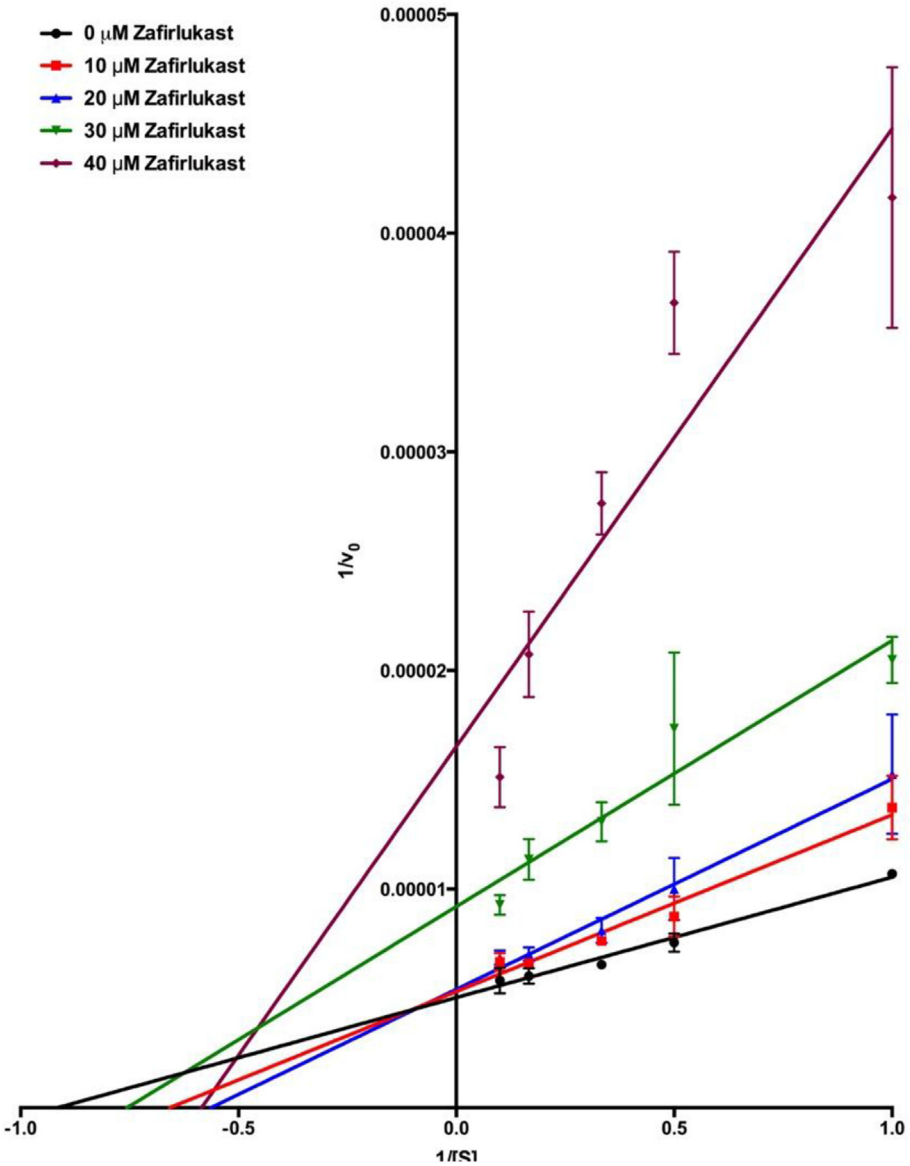

Fig. 3. Lineweaver-burk plot of WNV NS2B-NS3 protease with concentrations of zafirlukast at 0 (•), 10 (■), 20 (▲), 30 (▼), 40 (◆) μM. Substrate concentrations of 1, 2, 3, 6 and 10 μM for each inhibitor concentration.

would weaken it, which is observed experimentally.

Zafirlukast also contains a cyclopentyl carbamate connected at the C-5 of the indole. Removal of the cyclopentyl carbamate (**5**) resulted in poor inhibition and replacement of the cyclopentyl to an ethyl (**6**) gave similar poor inhibition as **5**. Substitution of the carbamate for an amide (**7**) also lowered inhibition. These results indicate the cyclopentyl group is occupying a hydrophobic binding site. This particular binding site is able to accommodate the cyclopentyl group, which suggests the site is relatively large. To further probe the size and hydrophobic nature of the binding site the cyclopentyl was replaced with a phenyl (**8**). This analog displayed better inhibition than zafirlukast with an IC_{50} of 22 μM. The phenyl group is larger than cyclopentyl, however it is planar and can participate in pi-stacking, which would increase interactions with aromatic residues leading to improved binding and inhibition. The carbamate functional group was also revealed to be important for binding, as removal of this group (**7**) lowered inhibition. The carbamate can participate in hydrogen bonding between the carbonyl of the carbamate and polar residues in the active site. The amide analog could also participate in the same interaction, but at a lesser degree than the carbamate resulting in weakened interactions leading to the lower inhibition, which is observed experimentally.

The overall shape of zafirlukast was investigated for inhibitor activity (Table 2.). The toluic acid-*N*-aryl sulfonamide moiety of Zafirlukast is connected at the C-2 of the indole. The moiety can also be connected at the N-1 of the indole to generate analogs with a different overall shape but does not restrict molecular rotation. Similar to the parent, when the toluic acid-*N*-aryl sulfonamide moiety or the *N*-aryl sulfonamide are removed (**9** and **10** respectively), there is effectively no inhibition. Interestingly when the toluic acid-*N*-aryl sulfonamide domain is attached to N-1 (**11**) the inhibitor activity is comparable to zafirlukast. This would suggest that the binding site occupied by zafirlukast is large and can accommodate the cyclopentyl carbamate and the toluic acid-N aryl sulfonamide domains in different molecular shapes. This evidence also supports the role of the indole core as a linker for the two domains. This theory was explored by synthesizing

Table 1
SAR of zafirlukast analogs (**1**–**8**).

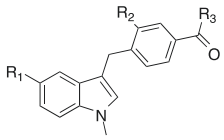

Cmpd	R_1	R_2	R_3	% Inhibition[a]
1		OMe	OMe	12
2		OMe		5
3		OMe	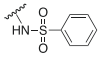	81
4		H	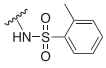	64
5	H	OMe	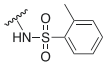	14
6		OMe	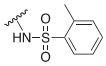	12
7	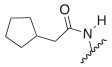	OMe	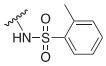	33
8	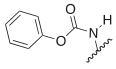	OMe	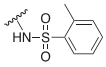	92

[a] At an inhibitor concentration of 60 μM.

Table 2
SAR of zafirlukast analogs (**9**–**11**).

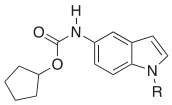

Cmpd	R	% Inhibition
9	CH_3	6
10	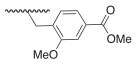	5
11	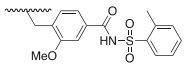	79

[a] At an inhibitor concentration of 60 μM.

analogs that contained a benzene linking the two domains. Two analogs were synthesized and examined for NS2B-NS3 protease inhibitor activity. Both analogs substituted the indole for a benzene with the cyclopentyl carbamate directly attached to the ring (Fig. 4). One analog did not contain the toluic acid moiety (**12**) resulting in minimal inhibition, which is consistent with previous experimental data. Compound **13** contained the toluic acid moiety linked to the benzene at the meta position, with moderate inhibition. It is concluded that **13** was better able to inhibit the NS2B-NS3 protease due to the spatial orientation of the two domains, with the benzene connecting the two groups at the meta position, resulting in an overall molecular shape similar to zafirlukast.

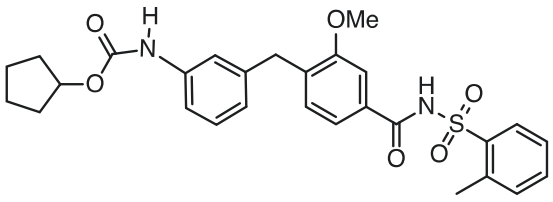

12: 30%

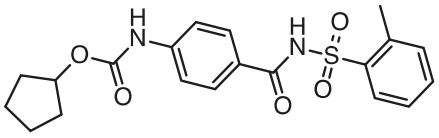

13: 4%

Fig. 4. Analogs of zafirlukast (**12** and **13**), replacing the indole core with a benzene. Percent inhibition at a concentration of 60 μM.

However, in the case of **12**, the benzene connects the two domains at the para position adopting a linear molecular shape and also lacked the toluic acid moiety, vastly different from zafirlukast. The experimental data indicates that the indole may not be essential for inhibition, however the overall molecular shape is vital for binding.

2.3. Molecular docking

To better understand how zafirlukast inhibits the viral protease, computational docking studies [29] of zafirlukast and **8** binding to the NS3 protein (PDB #2IJO) were conducted via Autodock Vina. Previously, researchers have proposed small molecules interacting with the NS3 protease at allosteric sites that would dislocate the NS2B cofactor from binding to the NS3 protein resulting in protease inhibition [13,25,26]. Disruption of the NS2B-NS3 complex has been experimentally proven to abate protease activity [8,30]. In addition, mutation of NS2B residues vital for binding to the NS3 protease also inactivated catalytic activity of the protease [31]. Therefore, the focus of our docking studies was to explore these allosteric sites on the NS3 protein to determine if they are viable binding sites for zafirlukast and **8**. There are three positions on the NS3 protein that have been identified as NS2B binding sites. One region is at the catalytic active site, another interface is located in proximity to Gln96 and the final binding site is adjacent to Phe116 of the NS3 protein [8,32]. The initial docking simulations were performed with the ligand binding site defined as the entire molecular surface of the NS3 protein to identify all favorable binding locations for zafirlukast. The results from this docking simulation revealed the lowest energy complex as zafirlukast binding to the NS3 protein in proximity to Phe116 as determined by AutoDock Vina scoring function (Fig. 5). A visual inspection of this lowest energy binding mode revealed zafirlukast interacting with two binding pockets. One pocket is formed by residues Phe116, Val154 Gly153 and Thr118 interacting with the phenyl sulfonamide (Fig. 6A). In this pocket there is pi-stacking observed between the phenyl sulfonamide and Phe116. In addition, there are other contacts between the phenyl sulfonamide and hydrophobic residues. The second pocket interacts with the cyclopentyl carbamate and is composed of Trp89, Ile147, Ile165, Lys88 and Gln167 (Fig. 6B). This binding site is hydrophobic with many contacts between the cyclopentyl

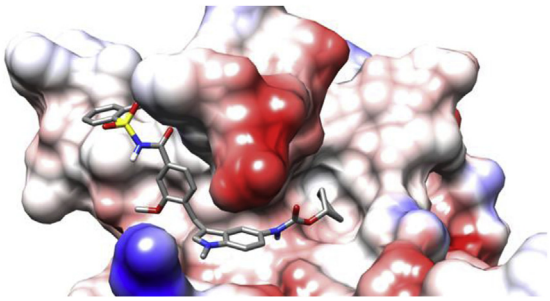

Fig. 5. Lowest energy binding mode between zafirlukast and NS3 protein via Autodock Vina.

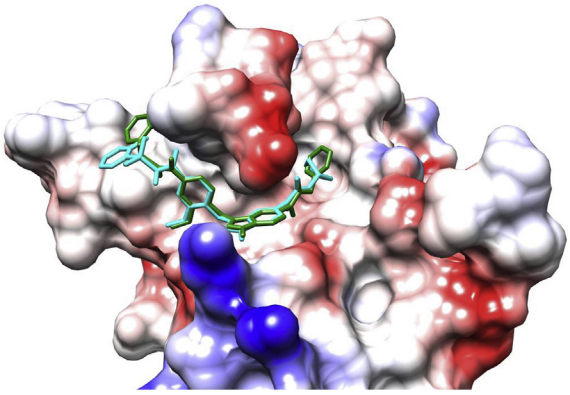

Fig. 7. Lowest energy docking complex for zafirlukast (teal) and **8** (green) superimposed on the NS3 protein. (For interpretation of the references to colour in this figure legend, the reader is referred to the Web version of this article.)

and hydrophobic residues including the carbon side chain of Lys88. Based on a visual inspection, both binding pockets could accommodate larger hydrophobic groups, particularly aromatic systems, which may improve binding and overall inhibition. The docking model also revealed Asn152 as a possible hydrogen bonding partner for the methoxy on the toluic acid. There is no hydrogen bonding observed in the docking complex, however rotation of the toluic acid could induce hydrogen bonding formation, which would explain the importance of the methoxy group in the SAR study. The indole core has hydrophobic contacts with Ile123 and the overall shape of zafirlukast formed by the connection of toluic *N*-aryl-sulfonamide and cyclopentyl carbamate domains at the indole C-2 and C-5 respectively, positions the domains into favorable binding sites.

Docking of **8** to the NS3 protein resulted in a similar binding model as zafirlukast, which is observed by superimposing the docked complex of zafirlukast and **8** on the NS3 protein (Fig. 7). Based on docking scores and supported by experimental inhibitor data, **8** is an improved binder than zafirlukast to the NS3 protein. The planar nature of the phenyl carbamate is better able to bind in the pocket, which has also improved the interactions of toluic acid and phenyl sulfonamide as both are interacting with Phe116, which is not observed in the zafirlukast docking complexes. These increased interactions improved binding and also resulted in greater disruption of NS2B binding. The docking models of zafirlukast and **8** are consistent with experimental data, indicating both domains are important for inhibitor activity. In both docking models the phenyl sulfonamide would be in position to disrupt NS2B binding resulting in NS2B-NS3 protease inhibition (Fig. 8). This supports experimental data implying that zafirlukast is inhibiting through a mixed mode inhibition due to binding at an allosteric site.

3. Chemistry

The initial syntheses centered on creating zafirlukast analogs with variations of the alkyl carbamate and *N*-aryl sulfonamide domains (Scheme 1). The indole nitrogen was methylated and underwent alkylation in the presence of silver oxide to give **17a-c** [27]. The nitro group was reduced to the amine and acylated to give the carbamate or amide precursors (**1**, **20a-d**) followed by hydrolysis of the methyl ester to give the corresponding carboxylic acid (**21a-21e**) as described in Table 3. The compounds were reacted with either the o-toluenesulfonamide, benzenesulfonamide or benzylamine to give the target compounds **2**–**4** and **6**–**8**. In addition, **5** and **9** were synthesized following similar reactions described in Scheme 1.

Analogs probing the molecular shape of zafirlukast were synthesized according to Scheme 2. Briefly, **14a** was alkylated at the N-1 of the indole with methyl-4-(bromomethyl)-3-methoxybenzoate followed by catalytic hydrogenation of the nitro to the corresponding amine (**23**) [28]. The amine was acylated with cyclopentyl chloroformate (**10**) and the toluate was hydrolyzed to toluic acid and coupled with o-toluenesulfonamide under EDC/DMAP conditions to give **11**.

The final compounds substituted the indole for a phenyl as depicted in Schemes 3 and 4. Compound **12** was synthesized beginning with a Suzuki coupling [33] between 3-nitrophenylboronic acid and methyl-4-(bromomethyl)-3-methoxybenzoate followed by reduction of the nitro to an amine (**26**). The amine was acylated with cyclopentyl chloroformate and

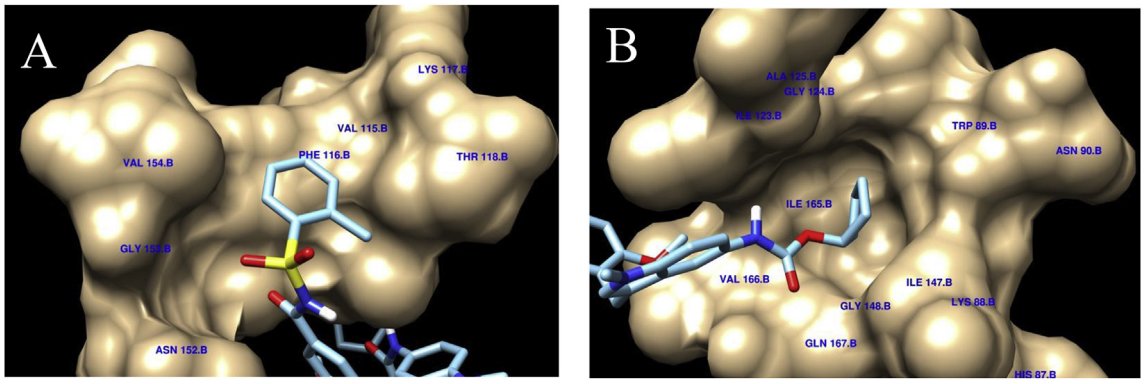

Fig. 6. Zafirlukast docked to the NS3 protein. A: NS3 protein binding pocket interacting with the phenyl sulfonamide and B: additional binding pocket interacting with cyclopentyl carbamate of zafirlukast.

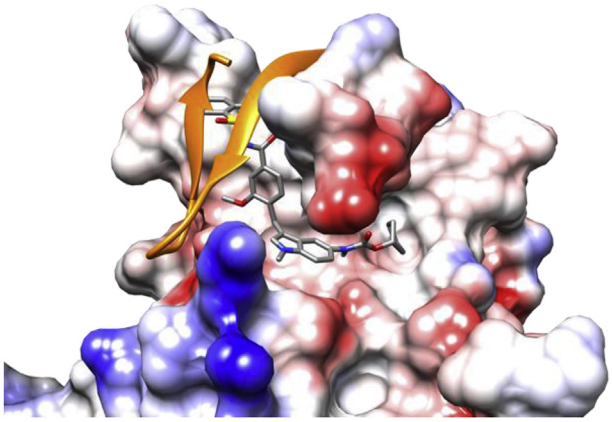

Fig. 8. Docking image of zafirlukast interfering with NS2B binding to the NS3.

the ester hydrolyzed and coupled with o-toluene sulfonamide to give **12**.

As indicated in Scheme 4, methyl 4-aminobenzoate was acylated with cyclopentyl chloroformate under basic conditions to give the cyclopentyl carbamate (**30**). The ester was hydrolyzed to the carboxylic acid and then coupled with o-toluene sulfonamide to yield **13.**

4. Conclusion

In summary, we report the discovery of zafirlukast as an inhibitor for the NS2B-NS3 protease. Zafirlukast was determined to inhibit the protease via a mixed mode mechanism with an IC_{50} value of 32 μM. The SAR study revealed the alkyl carbamate and *N*-toluic acid-*N*-aryl sulfonamide domains to be required for inhibition. Substituting the cyclopentyl with a phenyl improved inhibition with an IC_{50} value of 22 μM. An *in-silico* model of zafirlukast and **8** docked to the NS3 protein indicated binding at an allosteric site that disrupts formation of the NS2B-NS3 protease complex,

Table 3
Substitution pattern of compounds **14**–**21**.

Compound	R_1	R_2	R_3	R_4	Compound	R_1	R_2	R_3	R_4
14a	NO_2	–	–	–	**20a**	–	H		–
14b	H	–	–	–	**20b**	–	OMe		–
15a	NO_2	–	–	–	**20c**	–	OMe		–
15b	H	–	–	–	**20d**	–	OMe		–
17a	NO_2	H	–	–	**21a**	–	OMe		–
17b	NO_2	OMe	–	–	**21b**	–	H		–
17c	H	OMe	–	–	**21c**	–	OMe		–
19a	–	H	–	–	**21d**	–	OMe		–
19b	–	OMe	–	–	**21e**	–	OMe		–

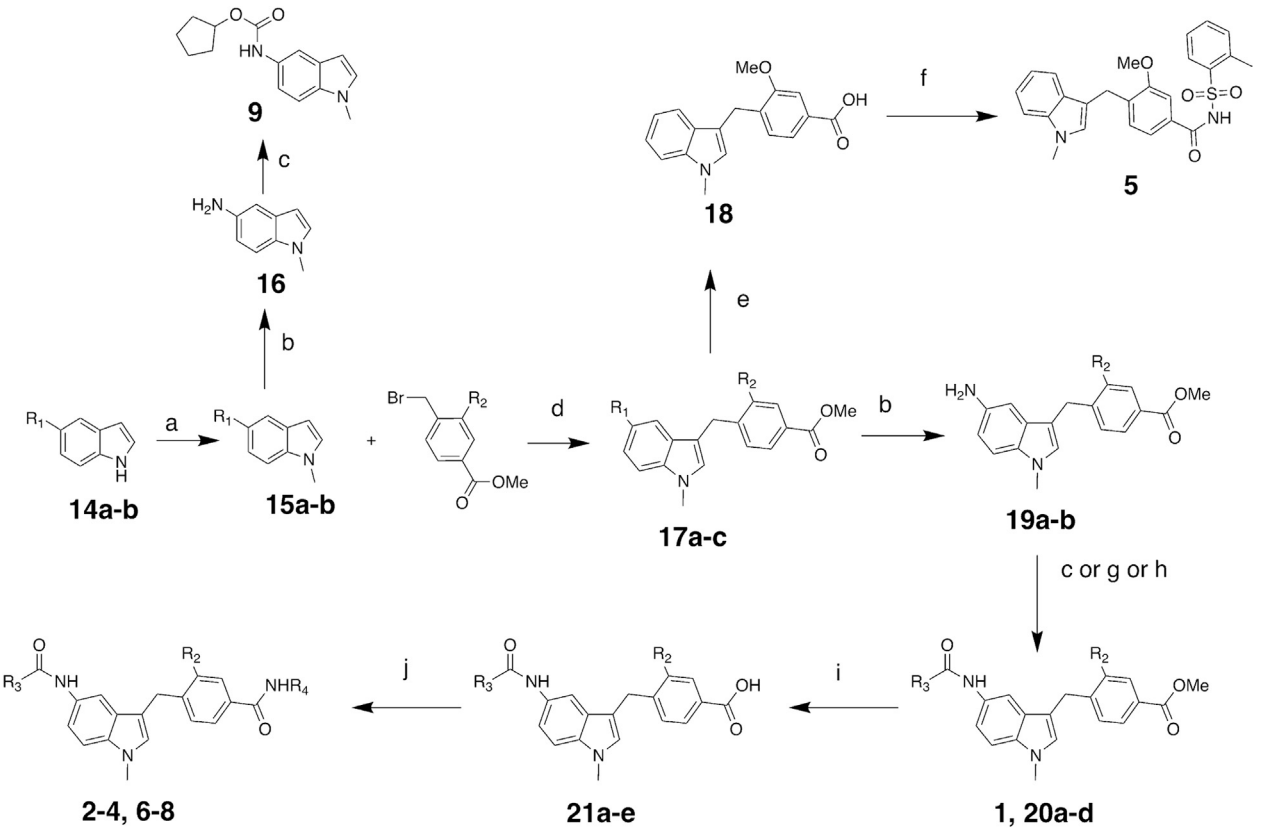

Scheme 1. Synthesis of **1**–**9**: a) MeI, acetone 40° C; b) H_2, 10% Pd/C, THF, 24–48 h; c) cyclopentyl chloroformate, $NaHCO_3$, THF/H_2O; d) Ag_2O, dioxane, 60° C, 20 h; g) cyclopentylacetic acid, DMAP, EDC, DCM, 16 h; g) ethyl chloroformate, $NaHCO_3$, THF/H_2O; i) 2 M NaOH aq., MeOH/THF, 60° C; j) benzylamine or o-toluene sulfonamide, DMAP, EDC, DCM, 16 h.

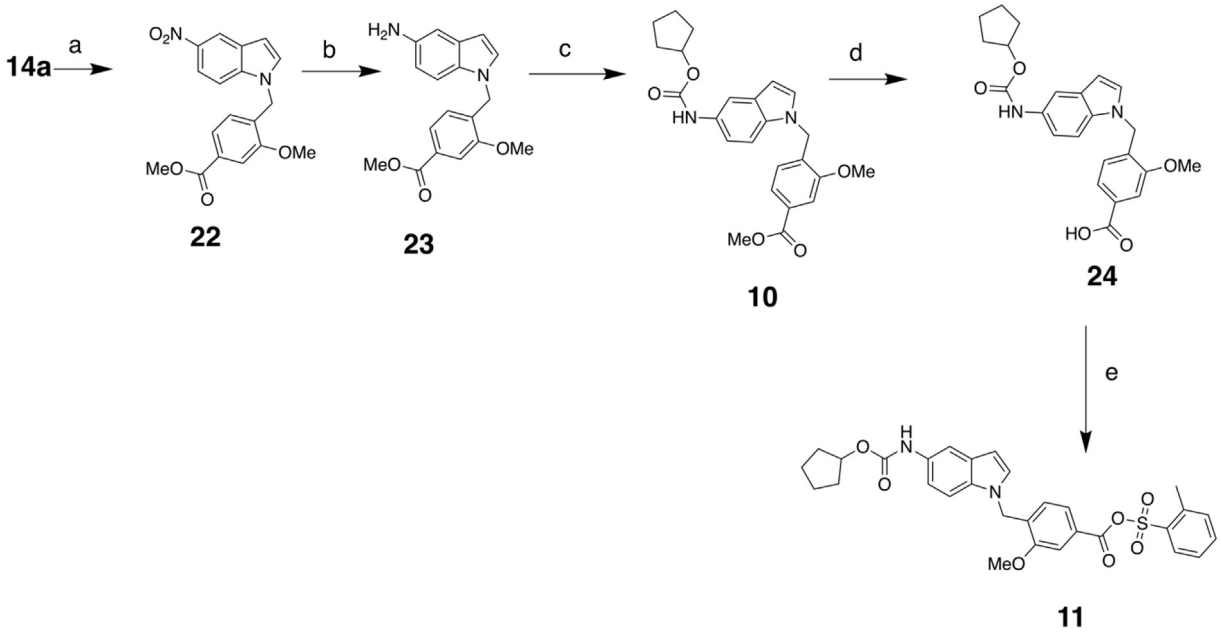

Scheme 2. Syntheses of **10** and **11**. a) methyl-4-(bromomethyl)-3-methoxybenzoate, NaH, DMF, RT, overnight; b) H_2, 10% Pd/C, THF, 24–48 h; c) cyclopentyl chloroformate, $NaHCO_3$, THF/H_2O; d) 2 M NaOH aq., MeOH/THF, 60° C; e) o-toluene sulfonamide, DMAP, EDC, DCM, 16 h.

thereby inhibiting catalytic activity, which is supported by experimental results. Future studies will continue to investigate the indole core and substitution of the indole with other privileged scaffolds to better orientate the carbamate and toluic acid-*N*-aryl sulfonamide domains for improved NS2B-NS3 protease inhibition.

5. Experimental section

5.1. Chemistry

5.1.1. Materials

All chemicals and reagents were obtained from Fisher Scientific and used without further purification. An authentic sample of zafirlukast was purchased from Fisher Scientific. Column chromatography was performed on a Teledyne Isco CombiFlash Rf+ with an EtOAc/Hex gradient utilizing RediSep Rf silica columns. NMR spectra was recorded utilizing a Bruker 400 MHz NMR operating at 400 MHz for proton NMR and 100 MHz for carbon NMR in either $CDCl_3$ or DMSO-d_6 solvent as indicated. High resolution mass spectra (HRMS) data was collected by a Q Exactive Focus mass spectrometer.

5.1.2. Synthetic procedures

All compounds were prepared following Schemes 1–4 based on literature procedures for the synthesis of zafirlukast and analogs.

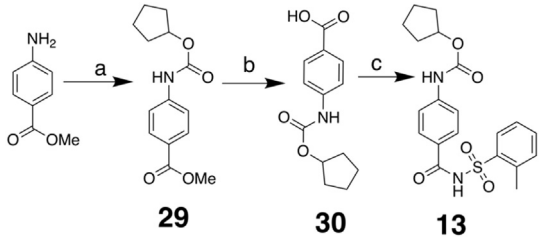

Scheme 4. Synthesis of 13. Reagents and conditions: a) cyclopentyl chloroformate, $NaHCO_3$, THF/H_2O; b) 2 M NaOH aq., MeOH/THF, 60° C; c) o-toluenesulfonamide, DMAP, EDC, DCM, 16 h.

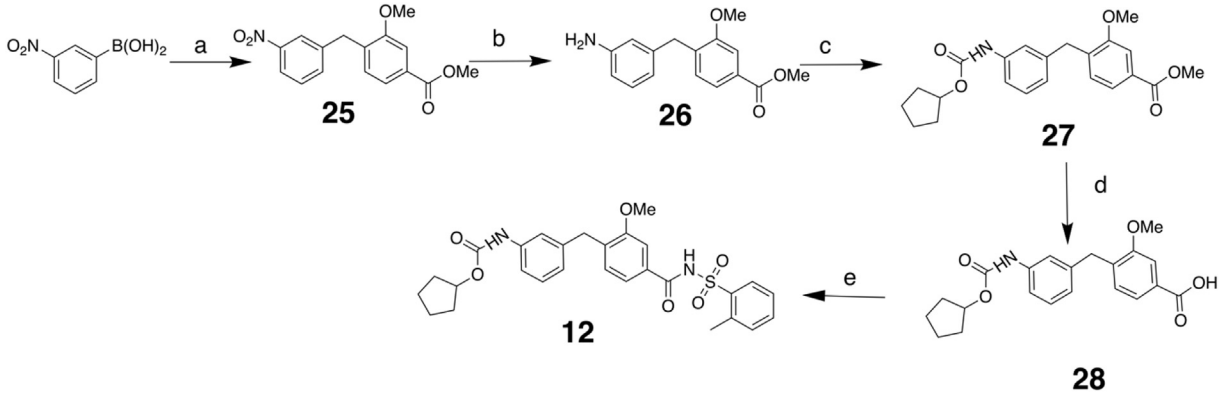

Scheme 3. Synthesis of **12**. Reagents and conditions: a) methyl-4-(bromomethyl)-3-methoxybenzoate, $CsCO_3$, $Pd(PPh_3)_4$, H_2O/DME, 90-100° C, 24 h; b) H_2, 10% Pd/C, THF, 24–48 h; c) cyclopentyl chloroformate, $NaHCO_3$, THF/H_2O; d) 2 M NaOH aq., MeOH/THF, 60° C e) o-toluenesulfonamide, DMAP, EDC, DCM, 16 h.

1-methyl-5-nitro-1H-indole **(15a):** KOH (5 eq.) was added to a solution of indole (1 eq.) dissolved in acetone (5 mL/mmol of indole) at 0 °C. Iodomethane (2 eq.) was added. Solution was stirred at 40 °C until disappearance of indole by TLC. Reaction was then cooled to room temperature. DCM (33 mL/mmol of indole) was added to reaction and stirred for 30 min. The solid was then filtered out and filtrate was washed 2 × H_2O, 1 × 1 M HCl, and 2 × H_2O. Organic layer was dried with Mg_2SO_4 and rotovapped. Crude product was recrystallized. Yellow solid; 65–100%; ^{1}H NMR ($CDCl_3$): δ8.61 (m, 1H), 8.16 (dd, 1H), 7.36 (dt, 1H), 7.23 (d, 1H), 6.70 (dd, 1H), 3.89 (s, 3H); ^{13}C NMR ($CDCl_3$): δ139.43, 132.00, 127.63, 118.18, 117.27, 109.08, 103.86, 99.99, 33.32.

*5.1.2.1. Compound **15b** was synthesized following the procedure described for **15a**.* 1-methyl-1H-indole (**15b**): Yellow oil; 50–100%; ^{1}H NMR (DMSO): δ7.66–7.56 (m, 1H), 7.47–7.39 (m, 1H), 7.31 (d, J = 3.2 Hz, 1H), 7.21 (ddd, J = 8.2, 6.9, 1.2 Hz, 1H), 7.16–7.02 (m, 1H), 6.51–6.41 (m, 1H), 3.77 (d, J = 0.9 Hz, 3H); ^{13}C NMR (DMSO): δ136.89, 129.94, 128.58, 121.48, 120.81, 119.38, 110.07, 100.76, 32.83;

Methyl 4-[(1-methyl-5-nitroindol-3-yl)methyl]benzoate **(17a):** Silver (I) oxide (1 eq.) was added to a stirred solution of indole (1 eq.) and benzyl bromide (1 eq.) in dioxane (1 mL/mmol of indole) in a microwave tube under nitrogen gas. The reaction was sealed and stirred at 60 °C for 20 h. EtOAc (2 mL/mmol of indole) was added to the reaction. The reaction was then filtered through celite and the filtrate was rotovapped. Product was purified by column chromatography to give a yellow solid; 25–45%; ^{1}H NMR (DMSO): δ8.42 (d, J = 2.3 Hz, 1H), 8.02 (dd, J = 9.1, 2.3 Hz, 1H), 7.93–7.84 (m, 2H), 7.60 (d, J = 9.1 Hz, 1H), 7.44 (d, J = 8.3 Hz, 3H), 4.21 (s, 2H), 3.83 (d, J = 4.1 Hz, 6H); ^{13}C NMR (DMSO): δ166.59, 147.18, 140.80, 140.05, 132.12, 129.82, 129.25, 127.93, 126.82, 116.99, 116.29, 116.03, 110.86, 52.45, 33.30, 30.65.

*5.1.2.2. Compounds **17b-c** were synthesized following the procedure described for **17a**.* Methyl 3-Methoxy-4-[(1-methyl-5-nitroindol-3-yl)methyl]benzoate. **(17b):** Yellow solid; 20–50%; ^{1}H NMR (DMSO): δ8.51 (d, 1H), 8.02 (dd, 1H), 7.59 (m, 1H), 7.49 (d, 2H), 7.38 (s, 1H), 7.29 (d, 1H), 4.12 (s, 2H), 3.86 (m, 9H); ^{13}C NMR (DMSO-d_6): δ166.56, 157.16, 140.76, 139.90, 135.10, 132.08, 130.38, 126.93, 122.07, 116.41, 115.56, 111.21, 110.81, 56.02, 52.57, 33.30, 24.94.

Methyl 3-methoxy-4-[(1-methyl-1H-indol-3-yl)methyl]benzoate **(17c):** Green oil; 40%; ^{1}H NMR (DMSO): δ7.57–7.31 (m, 4H), 7.24–7.04 (m, 3H), 6.98 (ddd, J = 8.0, 7.0, 1.0 Hz, 1H), 4.04 (s, 2H), 3.95–3.81 (m, 6H), 3.73 (s, 3H); ^{13}C NMR (DMSO): δ166.64, 157.22, 137.14, 135.81, 130.17, 129.07, 128.31, 127.83, 121.92, 121.53, 119.89, 119.07, 118.91, 111.91, 118.91, 111.91, 111.04, 110.05, 56.01, 52.51, 32.70, 25.17.

1-methyl-1H-indol-5-amine **(16)**: 10% Pd/C (0.18 g/g of starting material) was added to a solution of starting material dissolved in THF (54 mL/g of starting material). Reaction flask was sealed and vacuum was used to remove air. A balloon filled with hydrogen gas was then attached to the flask. The reaction was stirred at room temperature for 24–48 h or until disappearance of starting material was observed by TLC. The reaction was then filtered through celite. Filtrate was rotovapped to give a brown solid; 100%; ^{1}H NMR (DMSO): δ7.15–7.05 (m, 2H), 6.71 (dd, J = 3.0, 0.9 Hz, 1H), 6.57 (dd, J = 8.5, 2.1 Hz, 1H), 6.12 (dd, J = 3.0, 0.9 Hz, 1H), 3.67 (s, 3H); ^{13}C NMR (DMSO): δ141.30, 131.12, 129.49, 129.44, 129.41, 112.31, 110.11, 104.21, 99.13, 32.86.

*5.1.2.3. Compounds **19a,19b, 23, 26** were synthesized following the procedure described for **16**.* Methyl 4-[(5-amino-1-methyl-1H-indol-3-yl)methyl]benzoate **(19a):** brown solid; 50–70%; ^{1}H NMR (DMSO): δ7.90–7.82 (m, 2H), 7.41–7.33 (m, 2H), 7.11–7.03 (m, 1H), 6.96 (s, 1H), 6.56–6.48 (m, 2H), 4.47 (s, 2H), 3.99 (s, 2H), 3.82 (s, 3H), 3.63 (s, 3H); ^{13}C NMR (DMSO): δ166.68, 148.24, 141.51, 131.41, 129.63, 129.09, 128.55, 127.94, 127.56, 112.32, 110.69, 110.25, 102.27, 52.42, 32.69, 31.47.

4-[(5-amino-1-methyl-1H-indol-3-yl)methyl]-3-methoxy-*N*-(2-methylbenzenesulfonyl)benzamide **(19b):** A grey solid; 75%; ^{1}H NMR (DMSO): δ7.88 (dd, J = 7.7, 1.6 Hz, 1H), 7.50 (d, J = 1.5 Hz, 1H), 7.39 (dd, J = 7.7, 1.5 Hz, 1H), 7.34–7.13 (m, 4H), 7.09 (dd, J = 8.5, 0.6 Hz, 1H), 6.95 (d, J = 7.7 Hz, 1H), 6.86 (s, 1H), 6.65–6.52 (m, 2H), 5.60 (s, 3H), 3.84 (d, J = 4.0 Hz, 7H), 3.62 (s, 3H); ^{13}C NMR (DMSO): δ169.54, 156.54, 144.59, 139.82, 136.27, 131.75, 131.44, 130.39, 128.89, 128.12, 125.29, 120.93, 112.50, 110.84, 103.40, 55.68, 32.68, 25.10, 20.57.

Methyl 4-[(5-amino-1H-indol-1-yl)methyl]-3-methoxybenzoate **(23)**. Brown oil; 70%; ^{1}H NMR ($CDCl_3$): δ7.59 (d, J = 1.5 Hz, 1H), 7.49 (dd, J = 7.8, 1.6 Hz, 1H), 7.15–7.03 (m, 2H), 7.01–6.94 (m, 1H), 6.71–6.59 (m, 2H), 6.41 (dd, J = 3.1, 0.9 Hz, 1H), 5.31 (s, 2H), 3.95 (d, J = 23.7 Hz, 6H), 3.43 (s, 2H); ^{13}C NMR ($CDCl_3$): δ166.83, 156.41, 139.52, 131.56, 131.38, 130.46, 129.54, 128.95, 127.35, 122.18, 112.70, 110.79, 110.24, 105.79, 100.48, 55.61, 52.18, 45.16.

Methyl 4-[(3-aminophenyl)methyl]-3-methoxybenzoate **(26):** Yellow oil; 55%; ^{1}H NMR (DMSO): δ7.55–7.45 (m, 2H), 7.20 (d, J = 7.7 Hz, 1H), 6.90 (td, J = 7.2, 1.6 Hz, 1H), 6.41–6.31 (m, 3H), 4.94 (s, 2H), 3.88–3.77 (m, 8H); ^{13}C NMR (DMSO): δ166.62, 157.30, 149.11, 140.76, 135.73, 130.72, 129.26, 121.96, 116.86, 114.73, 112.27, 111.16, 56.03, 52.55, 35.66.

Methyl 4-[(5- [27]-1-methyl-1H-indol-3-yl)methyl]-3-methoxybenzoate **(1):** $NaHCO_3$ (3.1 eq.) and chloroformate (1.1 eq.) were added to a solution of amine (1 eq.) in THF (3.1 mL/mmol of amine) and H_2O (3.1 mL/mmol of amine). The reaction was stirred at room temperature until disappearance of amine was observed by TLC. The reaction was washed 3 × EtOAc. Combined organic layer was dried with Mg_2SO_4 and rotovapped. White oil; 60–90%; ^{1}H NMR (DMSO): δ9.21 (s, 1H), 7.60 (s, 1H), 7.52–7.42 (m, 2H), 7.27 (d, J = 8.6 Hz, 1H), 7.14 (d, J = 7.8 Hz, 2H), 7.05 (s, 1H), 5.06 (td, J = 6.0, 2.9 Hz, 1H), 3.94 (d, J = 16.8 Hz, 5H), 3.83 (s, 3H), 3.69 (s, 3H), 1.85 (d, J = 6.9 Hz, 1H), 1.67 (s, 4H), 1.57 (s, 3H); ^{13}C NMR (DMSO): δ166.65, 157.19, 154.14, 135.72, 133.73, 129.95, 129.02, 128.93, 127.70, 121.90, 111.42, 110.93, 109.95, 76.68, 56.00, 52.51, 35.47, 32.82, 32.77, 25.14, 23.72, 23.40; HRMS: $C_{25}H_{28}N_2O_5$ Calculated [M+H]: 437.2071 Observed: 437.2066.

*5.1.2.4. Compounds **9, 10, 20a, 20b, 20d, 27 and 29** were synthesized following the procedure described for **1**.* Cyclopentyl-*N*-(1-methyl-1H-indol-5-yl)carbamate **(9)**: Brown solid; 85%; ^{1}H NMR (DMSO): δ9.26 (s, 1H), 7.67 (s, 1H), 7.34–7.16 (m, 3H), 6.33 (dd, J = 3.0, 0.8 Hz, 1H), 5.09 (tt, J = 5.9, 2.8 Hz, 1H), 3.33 (s, 3H), 1.96–1.77 (m, 2H), 1.78–1.50 (m, 6H); ^{13}C NMR (DMSO): δ154.20, 133.40, 131.83, 130.44, 128.38, 114.72, 109.87, 100.44, 76.69, 32.94, 32.84, 23.75; HRMS: $C_{15}H_{18}N_2O_2$ Calculated [M+H]: 259.1441 Observed: 259.1442.

Methyl 4-[(5-{[(cyclopentloxy)carbonyl]amino}-1H-indol-1-yl) methyl]-3-methoxybenzoate **(10):** Brown solid; 74%; ^{1}H NMR ($CDCl_3$): δ7.73 (s, 1H), 7.58 (d, J = 1.5 Hz, 1H), 7.48 (dd, J = 7.9, 1.5 Hz, 1H), 7.22–7.08 (m, 3H), 6.64 (d, J = 7.9 Hz, 1H), 6.57–6.49 (m, 2H), 5.34 (s, 2H), 5.24 (tt, J = 6.1, 2.7 Hz, 1H), 3.97 (s, 3H), 3.91 (s, 3H), 1.99–1.56 (m, 8H); ^{13}C NMR ($CDCl_3$): δ166.77, 156.44, 133.43, 131.16, 130.61, 130.57, 129.32, 128.83, 127.36, 122.17, 110.86, 109.81, 101.70, 99.99, 77.74, 55.62, 52.18, 45.21, 32.81, 23.70; HRMS: $C_{24}H_{26}N_2O_5$ Calculated [M+H]: 423.1914 Observed: 423.1907.

Methyl 4-[(5-{[(cyclopentyloxy)carbonyl]amino}-1-methyl-1H-indol-3-yl)methyl]benzoate **(20a):** Purple solid; 90%; ^{1}H NMR (DMSO): δ9.21 (s, 1H), 7.91–7.83 (m, 2H), 7.57 (s, 1H), 7.42–7.34 (m, 2H), 7.31–7.24 (m, 1H), 7.14 (d, J = 28.3 Hz, 2H), 5.05 (tt, J = 5.3, 2.5 Hz, 1H), 4.05 (s, 2H), 3.82 (s, 3H), 3.70 (s, 3H), 1.88–1.79 (m, 2H), 1.69–1.53 (m, 6H); ^{13}C NMR (DMSO): δ166.66, 154.14, 147.87,

133.84, 129.69, 129.10, 128.85, 127.66, 127.50, 112.17, 110.01, 76.67, 52.43, 32.83, 32.79, 31.28, 23.73.

Methyl 4-({5-[(ethoxycarbonyl)amino]-1-methyl-1H-indol-3-yl}methyl)-3-methoxybenzoate **(20b):** Brown solid; 64%; ^{1}H NMR ($CDCl_3$): δ7.61–7.49 (m, 2H), 7.22–7.16 (s, 3H), 6.78 (s, 1H), 6.66 (s, 1H), 4.23 (q, J = 7.1 Hz, 2H), 4.09 (s, 2H), 3.93 (d, J = 11.0 Hz, 6H), 3.71 (s, 3H), 1.32 (t, J = 7.1 Hz, 3H); ^{13}C NMR ($CDCl_3$): δ167.23, 157.11, 154.36, 135.49, 134.35, 129.88, 129.65, 129.03, 128.22, 128.06, 122.02, 115.37, 112.54, 110.87, 110.41, 109.36, 60.92, 55.58, 52.03, 32.72, 25.24, 14.65.

Methyl 3-methoxy-4-({1-methyl-5-[(phenoxycarbonyl)amino]-1H-indol-3-yl}methyl)benzoate **(20d):** White solid; 46%; ^{1}H NMR ($CDCl_3$): δ7.69 (s, 1H), 7.55 (d, J = 7.7 Hz, 2H), 7.45–7.35 (m, 2H), 7.31–7.13 (m, 5H), 6.97 (s, 1H), 6.81 (s, 1H), 4.09 (s, 2H), 3.93 (d, J = 9.6 Hz, 6H), 3.74 (s, 3H); ^{13}C NMR ($CDCl_3$): δ167.22, 157.10, 150.88, 135.39, 129.60, 129.32, 129.06, 128.41, 128.10, 125.43, 122.02, 121.72, 112.67, 110.87, 109.50, 99.99, 55.59, 52.03, 32.76, 25.22.

Methyl 4-[(3-{[(cyclopentyloxy)carbonyl]amino}phenyl]-3-methoxybenzoate **(27):** Yellow oil; 100%; ^{1}H NMR (DMSO): δ9.46–9.41 (m, 1H), 7.55–7.44 (m, 2H), 7.34–7.10 (m, 4H), 6.85–6.78 (m, 1H), 5.05 (tt, J = 5.3, 2.4 Hz, 1H), 3.93–3.82 (m, 8H), 1.91–1.78 (m, 2H), 1.74–1.51 (m, 6H); ^{13}C NMR (DMSO): δ166.58, 157.34, 153.76, 140.83, 139.81, 135.23, 130.74, 129.48, 129.05, 123.16, 122.03, 118.94, 116.42, 111.23, 77.03, 56.05, 52.57, 35.76, 32.76, 23.70.

Methyl 4-{[(cyclopentyloxy)carbonyl]amino}benzoate **(29):** White solid; 80%; ^{1}H NMR (DMSO): δ9.98 (s, 1H), 7.92–7.81 (m, 2H), 7.64–7.55 (m, 2H), 5.11 (tt, J = 5.9, 2.8 Hz, 1H), 3.81 (s, 3H), 1.94–1.80 (m, 2H), 1.77–1.54 (m, 6H); ^{13}C NMR (DMSO): δ166.34, 153.61, 144.39, 130.76, 123.45, 117.82, 77.65, 52.27, 32.73, 23.71.

Methyl 4-{[5-(2-cyclopentylacetamido)-1-methyl-1H-indol-3-yl]methyl}-3-methoxybenzoate **(20c):** Carboxylic acid (1 eq.), DMAP (1.5 eq.), EDC (1.2 eq.), and amine (1.2 eq.) were added to DCM (10 mL/mmol of carboxylic acid) in that order. The reaction was stirred at room temperature for 16 h 2 M HCl was added to the reaction. Organic layer was extracted 3 × EtOAc. Combined organic layers were washed with brine. Organic layer was dried with Mg_2SO_4 and rotovapped. Product was purified by column chromatographyPink solid; 60%; ^{1}H NMR (DMSO): δ9.61 (s, 1H), 7.78–7.72 (m, 1H), 7.52–7.42 (m, 2H), 7.33–7.22 (m, 2H), 7.13 (d, J = 7.8 Hz, 1H), 7.06 (s, 1H), 3.98 (s, 2H), 3.93 (s, 3H), 3.83 (s, 3H), 3.70 (s, 3H), 2.19–2.03 (m, 1H), 1.81–1.68 (m, 3H), 1.68–1.42 (m, 4H), 1.26–1.04 (m, 3H); ^{13}C NMR (DMSO): δ174.50, 170.64, 166.64, 157.20, 135.72, 134.00, 131.76, 129.93, 129.04, 128.97, 127.57, 121.90, 115.43, 111.54, 110.93, 109.82, 109.70, 55.99, 52.51, 43.00, 37.23, 36.47, 32.78, 32.40, 25.15, 24.99.

3-methoxy-4-[(1-methyl-1H-indol-3-yl)methyl]benzoic acid **(18):** 2 M NaOH (11.1 mL/mmol of ester) was added to a solution of ester (1 eq.) in MeOH (11.1 mL/mmol of ester) and THF (5.55 mL/mmol of ester). The reaction was stirred at 60 °C until disappearance of ester was observed by TLC. 2 M HCl (11.1 mL/mmol of ester) was added to the reaction. The reaction was washed 3 × EtOAc. The combined organic layer was washed with brine. The organic layer was then dried with Mg_2SO_4 and rotovapped. White solid; 70%; ^{1}H NMR (DMSO): δ12.86 (s, 1H), 7.58–7.31 (m, 4H), 7.22–7.03 (m, 3H), 6.98 (ddd, J = 9.0, 6.9, 1.0 Hz, 1H), 4.01 (s, 2H), 3.90 (s, 3H), 3.73 (s, 3H); ^{13}C NMR (DMSO) δ167.73, 157.12, 137.12, 135.26, 130.23, 130.07, 128.27, 127.83, 122.04, 121.52, 119.09, 118.90, 112.07, 111.25, 110.04, 55.93, 32.70, 25.15.

*5.1.2.5. Compounds **21a-21e, 24 28 and 30** were synthesized following the procedure described for **18**.* 4-[(5- [27]-1-methyl-1H-indol-3-yl)methyl]-3-methoxybenzoic acid **(21a)** White solid; 40–75%; ^{1}H NMR (DMSO): δ12.03 (s, 1H), 9.22 (s, 1H), 7.61 (s, 1H), 7.55 (d, J = 2.8 Hz, 1H), 7.51–7.41 (m, 1H), 7.31–7.23 (m, 1H), 7.13 (d, J = 8.4 Hz, 2H), 7.04 (d, J = 2.5 Hz, 1H), 5.05 (d, J = 5.0 Hz, 1H), 3.98–3.88 (m, 5H), 3.69 (t, J = 2.1 Hz, 3H), 1.84 (d, J = 13.4 Hz, 2H), 1.66 (d, J = 12.8 Hz, 4H), 1.57 (s, 2H); ^{13}C NMR ($CDCl_3$): δ171.50, 157.13, 136.36, 134.32, 129.98, 129.69, 128.39, 128.23, 128.05, 122.77, 112.38, 111.21, 109.34, 99.99, 74.16, 55.58, 35.49, 32.82, 32.71, 25.29, 23.67, 23.29.

4-[(5-{[(cyclopentyloxy)carbonyl]amino}-1-methyl-1H-indol-3-yl)methyl]benzoic acid **(21b):** Purple solid; 40%; ^{1}H NMR (DMSO): δ12.73 (s, 1H), 9.21 (s, 1H), 7.89–7.80 (m, 2H), 7.58 (s, 1H), 7.39–7.32 (m, 2H), 7.28 (d, J = 8.7 Hz, 1H), 7.11 (s, 1H), 5.06 (tt, J = 4.9, 2.3 Hz, 1H), 4.04 (s, 2H), 3.70 (s, 3H), 1.84 (dd, J = 12.1, 5.7 Hz, 2H), 1.70–1.53 (m, 6H); ^{13}C NMR (DMSO): δ167.74, 154.14, 147.33, 133.83, 129.84, 128.90, 128.80, 127.52, 112.31, 109.99, 90.16, 76.68, 32.83, 32.78, 31.27, 23.73.

4-({5-[(ethoxycarbonyl)amino]-1-methyl-1H-indol-3-yl}methyl)-3-methoxybenzoic acid **(21c):** Brown solid; 84%; ^{1}H NMR ($CDCl_3$): δ7.74–7.56 (m, 2H), 7.32 (s, 1H), 7.32–7.17 (m, 2H), 7.04 (d, J = 9.2 Hz, 1H), 6.84 (s, 1H), 4.12 (s, 2H), 3.94 (s, 3H), 3.79–3.60 (m, 5H), 1.69–1.54 (m, 3H); ^{13}C NMR ($CDCl_3$): δ170.93, 157.12, 156.66, 135.86, 135.75, 129.77, 128.80, 128.34, 128.02, 122.61, 121.61, 118.11, 112.92, 111.29, 109.51, 62.40, 55.58, 32.76, 25.37, 14.66.

4-{[5-(2-cyclopentylacetamido}-1-methyl-1H-indol-3-yl]methyl}-3-methoxybenzoic acid **(21d):** 70%; ^{1}H NMR (DMSO): δ12.80 (s, 1H), 9.62 (s, 1H), 7.79–7.73 (m, 1H), 7.51–7.40 (m, 2H), 7.36–7.23 (m, 2H), 7.14–7.03 (m, 2H), 3.97 (s, 2H), 3.91 (s, 3H), 3.70 (s, 3H), 2.30–2.17 (m, 4H), 1.74 (dd, 11.6, 5.5 Hz, 2H), 1.67–1.45 (m, 4H), 1.20 (dt, J = 12.3, 7.1 Hz, 1H); ^{13}C NMR (DMSO): δ170.67, 167.76, 157.11, 135.18, 134.02, 131.76, 130.24, 129.76, 128.91, 127.61, 122.04, 115.47, 111.74, 111.16, 109.78, 60.21, 55.89, 43.02, 37.25, 36.48, 32.74, 32.42, 25.15, 25.01.

3-methoxy-4-({1-methyl-5-[(phenoxycarbonyl)amino]-1H-indol-3-yl}methyl)benzoic acid **(21e):** Brown solid; 33%; ^{1}H NMR ($CDCl_3$): δ7.66–7.55 (m, 2H), 7.43 (s, 1H), 7.34–7.26 (m, 2H), 7.25–7.08 (m, 2H), 7.03 (s, 1H), 6.86 (d, J = 13.7 Hz, 1H), 6.71 (s, 3H), 4.15 (s, 2H), 3.94 (s, 3H), 3.74 (s, 3H); ^{13}C NMR ($CDCl_3$): δ157.15, 154.80, 151.54, 135.95, 132.99, 129.77, 129.06, 128.54, 128.08, 125.09, 122.68, 121.68, 121.40, 118.21, 112.95, 111.32, 109.70, 55.60, 32.79, 25.41.

4-[(5-{[(cyclopentyloxy)carbonyl]amino}-1H-indol-1-yl)methyl]-3-methoxybenzoic acid **(24):** Purple solid; 65%; ^{1}H NMR ($CDCl_3$): δ7.72 (s, 1H), 7.64–7.52 (m, 2H), 7.21–7.08 (m, 3H), 6.66 (d, J = 7.8 Hz, 1H), 6.57–6.50 (m, 2H), 5.36 (s, 2H), 5.27–5.20 (m, 1H), 3.98 (s, 3H), 1.99–1.59 (m, 8H); ^{13}C NMR ($CDCl_3$): δ170.81, 156.46, 133.45, 132.14, 130.54, 129.67, 129.33, 128.84, 127.40. 122.94, 128.84, 127.40, 122.94, 111.17, 109.78, 101.80, 99.99, 55.63, 45.25, 32.81, 23.69.

4-[(3-{[(cyclopentyloxy)carbonyl]amino)phenyl)methyl]-3-methoxybenzoic acid **(28):** White solid; 40%; ^{1}H NMR (DMSO): δ12.88 (s, 1H), 9.44 (s, 1H), 7.53–7.45 (m, 2H), 7.33–7.25 (m, 2H), 7.22–7.11 (m, 2H), 6.82 (dt, J = 7.6, 1.4 Hz, 1H), 5.06 (ddd, J = 6.7, 5.1, 1.9 Hz, 1H), 3.87 (d, J = 19.3 Hz, 5H), 1.84 (dp, J = 11.8, 8.3, 6.6 Hz, 3H), 1.74–1.51 (m, 5H); ^{13}C NMR (DMSO): δ157.24, 149.27, 140.99, 134.31, 130.58, 129.25, 123.17, 122.15, 118.71, 116.11, 111.45, 107.54, 98.06, 77.03, 55.97, 35.40, 32.76, 23.71.

4-{[(cyclopentyloxy)carbonyl]amino}benzoic acid **(30):** Pink solid; 60%; ^{1}H NMR (DMSO): δ12.59 (s, 1H), 9.92 (s, 1H), 7.91–7.81 (m, 2H), 7.63–7.53 (m, 2H), 5.11 (td, J = 5.9, 2.9 Hz, 1H), 1.96–1.80 (m, 2H), 1.77–1.52 (m, 6H); ^{13}C NMR (DMSO): δ167.43, 153.63, 144.00, 130.87, 124.62, 117.70, 77.58, 32.74, 23.7.

Cyclopentyl *N*-[1-methyl-3-({4-[(2-methylbenzenesulfonyl)carbamoyl]phenyl}methyl)-1H-indol-5-yl]carbamate **(2):** Carboxylic acid (1 eq.), DMAP (1.5 eq.), EDC (1.2 eq.), and amine/sulfonamide (1.2 eq.) were added to DCM (10 mL/mmol of carboxylic acid) in that order. The reaction was stirred at room temperature for 16 h 2 M HCl was added to the reaction. Organic layer was extracted 3 ×

EtOAc. Combined organic layers were washed with brine. Organic layer was dried with Mg_2SO_4 and rotovapped. Product was purified by column chromatography. Grey solid; 69%; ^{1}H NMR (DMSO): δ12.53 (s, 1H), 9.20 (s, 1H), 8.02 (d, J = 7.9 Hz, 1H), 7.80 (d, J = 8.0 Hz, 2H), 7.57 (t, J = 7.3 Hz, 2H), 7.48–7.23 (m, 5H), 7.13 (d, J = 27.9 Hz, 2H), 5.10–5.01 (m, 1H), 4.03 (s, 2H), 3.69 (s, 3H), 2.60 (s, 3H), 1.88–1.82 (m, 2H), 1.66 (s, 4H), 1.56 (s, 2H); ^{13}C NMR (DMSO): δ165.65, 154.14, 147.78, 137.30, 133.81, 132.76, 131.57, 130.82, 128.93, 128.88, 127.46, 126.61, 112.19, 110.01, 76.68, 32.83, 32.81, 23.73, 20.06; HRMS: $C_{30}H_{31}N_3O_6S$ Calculated [M+H]: 562.2006 Observed: 562.2007.

*5.1.2.6. Compounds **3**–**8** and **11**–**13** were synthesized following the procedure described for **2**.* Cyclopentyl *N*-[3-({4-[(benzenesulfonyl) carbamoyl]-2-methoxyphenyl}methyl)-1-methyl-1H-indol-5-yl] carbamate **(3):** Grey solid; 42%; ^{1}H NMR (DMSO): δ12.46 (s, 1H), 9.20 (s, 1H), 8.05–7.95 (m, 2H), 7.77–7.56 (m, 4H), 7.48 (d, J = 1.7 Hz, 1H), 7.38 (dd, J = 7.8, 1.7 Hz, 1H), 7.32–7.22 (m, 1H), 7.12 (dd, J = 18.4, 8.1 Hz, 2H), 7.02 (s, 1H), 5.05 (tt, J = 5.2, 2.5 Hz, 1H), 3.92 (s, 3H), 3.68 (s, 3H), 1.84–1.57 (m, 8H); ^{13}C NMR (DMSO): δ165.46, 157.11, 154.14, 139.98, 135.80, 134.10, 133.72, 130.58, 129.81, 129.57, 128.90, 128.12, 127.66, 121.19, 111.39, 110.53, 109.94, 76.68, 56.15, 32.82, 32.76, 25.13, 23.72; HRMS: $C_{31}H_{33}N_3O_4$ Calculated [M+H]: 512.2544 Observed: 512.2545.

Cyclopentyl *N*-[1-methyl-3-({3-[(2-methylbenzenesulfonyl)carbamoyl]phenyl}methyl)-1H-indol-5-yl]carbamate **(4):** Grey solid; 40%; ^{1}H NMR (DMSO): δ12.61 (s, 1H), 9.20 (s, 1H), 8.04 (dd, J = 8.0, 1.4 Hz, 1H), 7.80–7.68 (m, 2H), 7.58 (td, J = 7.3, 1.4 Hz, 2H), 7.54–7.35 (m, 4H), 7.27 (d, J = 8.7 Hz, 1H), 7.17 (d, J = 8.9 Hz, 1H) 7.06 (s, 1H), 5.06 (ddd, J = 7.0, 5.1, 2.0 Hz, 1H), 4.01 (s, 2H), 3.69 (s, 3H), 2.60 (s, 3H), 1.89–1.79 (m, 2H), 1.69–1.53 (m, 6H); ^{13}C NMR (DMSO): δ165.83, 154.16, 142.66, 138.00, 137.41, 134.00, 133.83, 133.62, 132.82, 131.89, 131.57, 130.94, 128.97, 128.78, 128.72, 127.46, 126.67, 126.30, 112.49, 110.00, 76.69, 32.83, 32.78, 30.98, 23.73, 20.04; HRMS: $C_{30}H_{31}N_3O_5S$ Calculated [M+H]: 546.2057 Observed: 546.2049.

3-methoxy-4-[(1-methyl-1H-indol-3-yl)methyl]-*N*-(2-methylbenzenesulfonyl)benzamide **(5)**: Tan solid; 50%; ^{1}H NMR (DMSO): δ12.56 (s, 1H), 8.05 (dd, J = 7.9, 1.4 Hz, 1H), 7.63–7.28 (m, 8H), 7.22–7.04 (m, 2H), 6.97 (ddd, J = 7.9, 7.0, 1.0 Hz, 1H), 4.01 (s, 2H), 3.91 (s, 3H), 3.35 (s, 3H), 2.51 (s, 3H); ^{13}C NMR (DMSO): δ165.29, 157.15, 138.04, 137.36, 137.12, 135.86, 134.01, 132.83, 130.96, 130.57, 130.04, 128.29, 127.78, 126.69, 121.52, 121.16, 119.06, 118.90, 111.89, 110.62, 110.05, 56.17, 32.69, 31.15, 25.15; HRMS: $C_{25}H_{24}N_2O_4S$ Calculated [M+H]: 449.1530 Observed: 449.1522.

Methyl 4-({5-[(ethoxycarbonyl)amino]-1-methyl-1H-indol-3-yl}methyl)-3-methoxybenzoate **(6):** Brown solid; 64%; ^{1}H NMR ($CDCl_3$): δ7.61–7.49 (m, 3H), 6.78 (s, 1H), 6.66 (s, 1H), 4.23 (q, J = 7.1 Hz, 2H), 4.09 (s, 2H), 3.93 (d, J = 11.0 Hz, 6H), 3.71 (s, 3H), 1.32 (t, J = 7.1 Hz, 3H); ^{13}C NMR ($CDCl_3$): δ167.23, 157.11, 154.36, 135.49, 134.35, 129.88, 129.65, 129.03, 128.22, 128.06, 122.02, 115.37, 112.54, 110.87, 110.41, 109.36, 60.92, 55.58, 52.03, 32.72, 25.24, 14.65; HRMS: $C_{28}H_{29}N_3O_6S$ Calculated [M+H]: 536.1850 Observed: 536.1844.

*5.1.2.7. 4-{[5-(2-cyclopentylacetamido}-1-methyl-1H-indol-3-yl] methyl}-3-methoxybenzoic acid **(7)**.* Grey solid; 70%; ^{1}H NMR (DMSO): δ12.80 (s, 1H), 9.62 (s, 1H), 7.79–7.73 (m, 1H), 7.51–7.40 (m, 2H), 7.36–7.23 (m, 2H), 7.14–7.03 (m, 2H), 3.97 (s, 2H), 3.91 (s, 3H), 3.70 (s, 3H), 2.30–2.17 (m, 4H), 1.74 (dd, 11.6, 5.5 Hz, 2H), 1.67–1.45 (m, 4H), 1.20 (dt, J = 12.3, 7.1 Hz, 1H); ^{13}C NMR ($CDCl_3$): δ171.50, 157.13, 136.36, 134.32, 129.98, 129.69, 128.39, 128.23, 128.05, 122.77, 112.38, 111.21, 109.34, 99.99, 74.16, 55.58, 35.49, 32.82, 32.71, 25.29, 23.67, 23.29δ; HRMS: $C_{32}H_{35}N_3O_5S$ Calculated [M+H]: 574.2370 Observed: 574.2371.

Phenyl *N*-[3-([2-methoxy-4-[(2-methylbenzenesulfonyl)carbamoyl]phenyl}methyl)-1-methyl-1H-indol-5-yl]carbamate **(8):** Grey solid; 20%; ^{1}H NMR (DMSO): δ12.57 (s, 1H), 9.94 (s, 1H), 8.03 (dd, J = 8.0, 1.4 Hz, 1H), 7.67–7.53 (m, 2H), 7.55–7.30 (m, 7H), 7.29–7.04 (m, 7H) 3.93 (d, J = 21.3 Hz, 6H), 3.71 (s, 3H), 2.51 (s, 2H); ^{13}C NMR (DMSO): δ165.36, 157.11, 152.44, 151.25, 138.16, 137.33, 135.66, 134.00, 132.80, 130.91, 130.83, 129.83, 129.79, 129.16, 127.69, 126.66, 125.62, 122.43, 121.14, 114.92, 111.60, 110.55, 110.19, 109.08, 56.16, 32.81, 25.10, 20.04; HRMS: $C_{32}H_{29}N_3O_6S$ Calculated [M+H]: 584.1850 Observed: 584.1841.

Cyclopentyl *N*-[1-({2-methoxy-4-[(2-methylbenzenesulfonyl) carbamoyl]phenyl}methyl)-1H-indol-5-yl]carbamate **(11):** White solid; 5%; ^{1}H NMR (DMSO): δ12.61 (s, 1H), 9.24 (s, 1H), 8.02 (d, J = 7.7 Hz, 1H), 7.68 (s, 1H), 7.61–7.50 (m, 2H), 7.48–7.32 (m, 4H), 7.24 (d, J = 8.8 Hz, 1H), 7.16–7.09 (m, 1H), 6.66 (d, J = 7.9 Hz, 1H), 6.40 (d, J = 3.1 Hz, 1H), 5.35 (s, 2H), 5.07 (dt, J = 6.4, 3.4 Hz, 1H), 3.93 (s, 3H), 2.59 (s, 3H), 1.71–1.55 (m, 8H); ^{13}C NMR (DMSO): δ156.74, 154.19, 132.80, 132.05, 130.27, 128.55, 127.92, 126.60, 121.17, 110.81, 110.23, 101.33, 76.71, 56.28, 44.73, 32.28, 23.74, 20.05; HRMS: $C_{30}H_{31}N_3O_6S$ Calculated [M+H]: 562.2006 Observed: 562.2000.

Cyclopentyl *N*-[3-({2-methoxy-4-[(2methylbenzenesulfonyl) carbamoyl]phenyl}methyl)phenyl]carbamate **(12):**White solid; 35% ^{1}H NMR (DMSO): δ12.60 (s, 1H), 9.43 (s, 1H), 8.08–8.01 (m, 1H), 7.64–7.55 (m, 1H), 7.53–7.37 (m, 4H), 7.27 (d, J = 13.5 Hz, 2H), 7.22–7.10 (m, 2H), 6.80 (d, J = 7.6 Hz, 1H), 5.06 (dt, J = 5.9 Hz, 2.6 Hz, 1H), 3.86 (d, J = 9.9 Hz, 5H), 2.62 (s, 3H), 1.84 (d, J = 8.7 Hz, 3H), 1.66 (s, 3H), 1.57 (t, J = 5.7 Hz, 2H); ^{13}C NMR (DMSO): δ165.22, 157.27, 153.76, 140.81, 139.80, 138.00, 137.37, 135.27, 134.03, 132.85, 130.98, 130.95, 130.62, 129.04, 126.70, 123.15, 121.27, 118.93, 116.44, 110.82, 77.04, 56.21, 35.74, 32.76, 23.70, 20.04; HRMS: $C_{28}H_{30}N_2O_6S$ Calculated [M+H]: 523.1897 Observed: 523.1889.

Cyclopentyl *N*-{4-[(2-methylbenzenesulfonyl)carbamoyl] phenyl}carbamate **(13):** White solid; 35%; ^{1}H NMR (DMSO): δ12.60 (s, 1H), 9.43 (s, 1H), 8.08–8.01 (m, 1H), 7.64–7.55 (m, 1H), 7.53–7.37 (m, 4H), 7.27 (d, J = 13.5 Hz, 2H), 7.22–7.10 (m, 2H), 6.80 (d, J = 7.6 Hz, 1H), 5.06 (dt, J = 5.9 Hz, 2.6 Hz, 1H), 3.86 (d, J = 9.9 Hz, 5H), 2.62 (s, 3H), 1.84 (d, J = 8.7 Hz, 2H), 1.66 (s, 3H), 1.57 (t, J = 5.7 Hz, 2H); ^{13}C NMR (DMSO): δ165.22, 157.27, 153.76, 140.81, 139.80, 138.00, 137.37, 135.27, 134.03, 132.85, 130.98, 130.95, 130.62, 129.04, 126.70, 123.15, 121.27, 118.93, 116.44, 110.82, 77.04, 56.21, 35.74, 32.76, 23.70, 20.04; HRMS: $C_{28}H_{30}N_2O_6S$ Calculated [M+H]: 521.1752 Observed: 521.1692.

Methyl 4-[(5-nitro-1H-indol-1-yl)methyl]-3-methoxybenzoate **(22):** NaH (1.08 eq.) was added dropwise to indole (1 eq.) dissolved in DMF (4 mL/mmol of indole) at 0 °C. The solution was stirred for 30 min at room temperature. The halide (1 eq.) was added portionwise at 0 °C. The solution was then stirred overnight at room temperature. The reaction was then washed 3 × EtOAc. The combined organic layer was then washed with brine. Organic layer was dried with Mg_2SO_4 and rotovapped. Product was purified by column chromatography. Tan solid; 50%; ^{1}H NMR (DMSO): δ8.60 (d, J = 2.3 Hz, 1H), 8.01 (dd, J = 9.1, 2.3 Hz, 1H), 7.74–7.60 (m, 2H), 7.56–7.44 (m, 2H), 6.89 (d, J = 7.9 Hz, 1H), 6.82 (dd, J = 3.2, 0.8 Hz, 1H), 5.54 (s, 2H), 3.93 (s, 3H), 3.84 (s, 3H); ^{13}C NMR (DMSO): δ166.30, 157.07, 141.35, 139.34, 133.64, 131.03, 130.95, 128.52, 127.89, 122.08, 118.08, 117.07, 111.42, 111.11, 104.53, 56.72, 52.71, 45.34.

Methyl 4-[(3-nitrophenyl)methyl]-3-methoxybenzoate **(25):** Cs_2CO_3 (2 eq.) was dissolved in H_2O (2 mL/mmol halide) and degassed. Halide (1 eq.), $Pd(PPh_3)_4$ (0.2 eq), and boronic acid (1 eq.) was added in that order to DME (4 mL/mmol of halide) in a microwave tube under argon gas. Cs_2CO_3/H_2O was then added to the solution. The microwave tube was then sealed and stirred at 90–100 °C for 24 h. The organic layer was then extracted 3 × H_2O/DCM. The organic layer was then dried with Mg_2SO_4 and rotovapped. Product was purified by column chromatography. White solid;

51%; ^{1}H NMR (DMSO): δ8.06 (tdd, J = 3.6, 2.4, 1.1 Hz, 2H), 7.72–7.47 (m, 4H), 7.38 (d, J = 7.8 Hz, 1H), 4.12 (s, 2H), 3.85 (d, J = 1.9 Hz, 6H); ^{13}C NMR (DMSO): δ166.48, 157.38, 148.77, 142.78, 135.99, 134.08, 131.00, 130.30, 130.04, 123.55, 122.20, 121.65, 111.45, 56.11, 52.63, 35.11.

5.2. Enzymatic assay

The FRET assay was performed in Costar black 96-well plates with buffer A (10 mM Tris-HCl, 20% glycerol, 0.005% tween at a pH of 7.97) and monitored with a Molecular Devices SpectraMax M2^{e} plate reader running SoftMax Pro 6.1 software. The WNV NS2B-NS3 protease was expressed and purified following literature procedures and the substrate for the assay was synthesized as previously described [24].

5.2.1. Determination of percent inhibition

The FRET assay was performed in 96-well plates with NS2B-NS3 protease (8 nM) in buffer A and compounds of interest were dissolved in DMSO and added to the wells at a final concentration of 60 μM. The enzymatic reaction was initiated by the addition of substrate (10 μM) and monitored by the plate reader for 20 min with fluorescence measurements (excitation = 325 nm, emission = 400 nm) collected every 30 s. The initial slopes of the enzymatic reactions (0–3 min) RFU/sec were compared to control reactions (no inhibitor) to determine percent inhibition. The enzymatic assays for each compound was performed in triplicate.

5.2.2. Determination of IC_{50} values

The FRET assay was performed for each compound (enzyme 10 nM, substrate 10 μM and inhibitor concentrations of 5, 15, 30, 45, 60, 75 and 90 μM) with buffer A. The initial enzymatic rate of reaction was determined at each inhibitor concentration. The rates (RFU/second) at different concentrations were normalized to the rate of the control. The log (inhibitor) vs. normalized response – variable rate model was used to calculate the IC_{50} using Prism 6.0 (Graftpad, San diego, CA).

5.2.3. Lineweaver-burk plot

The enzymatic assay was performed at a fixed enzyme concentration of 10 nM with a mixed matrix of substrate (1, 2, 3, 6, and 10 μM) and zafirlukast concentrations (10, 20, 30, 40, 50, 60, 70, and 80 μM) in buffer A. The enzymatic reactions were initiated by the addition of substrate and the reaction was monitored for 10 min, measuring fluorescence (excitation = 325 nm, emission = 400 nm) every 30 s. The initial rate of the reaction was determined by measuring the slope of the RFU versus time during 1 min–2:30 min of the enzymatic reaction. The inverse of the initial enzymatic rate vs the inverse of the substrate concentrations was plotted for each inhibitor concentration with Prism 6.0 (Graftpad, San Diego, CA).

5.2.4. Enzymatic assay with detergents

Reaction mixtures (100 μl) contained 30 nM NS2B-NS3 protease, 20 μM FRET substrate, 50 μM Zafirlukast, indicated percentages (0.01, 0.05, 0.1 and 0.2) of Brij35 and CHAPS detergent, and Buffer A (10 mM Tris HCl pH 8.0, 20% glycerol and 0.005% tween). DMSO was used as the control. Reactions were initiated by adding the protease to reaction mixtures and absorbance measurements were collected immediately every 30 s for a total of 5 min to calculate the initial velocity. Each bar graph is the average of three separate experiments and standard error is indicated.

5.3. Molecular docking

Molecular docking was performed using Autodock Vina (The Scripps Research Institute, La Jolla, CA) on a Mac Book air computer running OS 10.12.6 with a 1.8 GHz Intel Core i5 processor. The solved X-ray crystal structure of WNV NS2B-NS3 protease (pdb # 2IJO) was used as a static receptor for docking. Both the co-crystalized ligand and NS2B were removed from the NS3 protein structure prior to docking. The initial docking of zafirlukast was performed with a search box located at x = −23.624, y = −3.111, z = 4.244 coordinates, with a search box size of 56 × 38 x 56 to allow zafirlukast to dock freely on the surface of the NS3 protein. The docking results were sorted by Autodock scoring function to identify the most favorable binding mode, which is shown in Figs. 5 and 6. Follow-up docking calculations were run on the NS3 protein with a search box located at x = 21.037, y = 1.849, z = 18.2 coordinates with a box size of 20.25 × 15 × 23.5 Å for both zafirlukast and **8** which was used to generate Figs. 7 and 8. The small molecule ligands were drawn using ChemDraw (Perkin Elmer) and minimized with Chem3D (Perkin Elmer). All docking images were generated by Chimera [34].

Funding sources

We are grateful to Allergan Foundation, California State University program in Education and Research in Biotechnology and California State University, Fullerton for financial support of this research. Instrumentation support was provided by Department of Defense (68816-RT-REP) and the National Science foundation MRI (CHE1726903) for acquisition of an UPLC-MS. Molecular graphics and analyses were performed with the UCSF Chimera package (supported by NIGMS P41-GM103311).

Appendix A. Supplementary data

Supplementary data related to this article can be found at https://doi.org/10.1016/j.ejmech.2018.08.077.

References

[1] T.M. Colpitts, M.J. Conway, R.R. Montgomery, E. Fikrig, West Nile Virus: biology, transmission, and human infection, Clin. Microbiol. Rev. 25 (2012) 635–648.
[2] E.B. Hayes, D.J. Gubler, West Nile virus: epidemiology and clinical features of an emerging epidemic in the United States, Annu. Rev. Med. 57 (2006) 181–194.
[3] J.T. Watson, P.E. Pertel, R.C. Jones, A.M. Siston, W.S. Paul, C.C. Austin, S.I. Gerber, Clinical characteristics and functional outcomes of West Nile fever, Ann. Intern. Med. 141 (2004) 360–365.
[4] S. Mukhopadhyay, R.J. Kuhn, M.G. Rossmann, A structural perspective of the flavivirus life cycle, Nat. Rev. Microbiol. 3 (2005) 13–22.
[5] T.J. Chambers, C.S. Hahn, R. Galler, C.M. Rice, Flavivirus genome organization, expression, and replication, Annu. Rev. Microbiol. 44 (1990) 649–688.
[6] G.L. Campbell, A.A. Marfin, R.S. Lanciotti, D.J. Gubler, West Nile virus, Lancet Infect. Dis. 2 (2002) 519–529.
[7] G. Robin, K. Chappell, M.J. Stoermer, S.-H. Hu, P.R. Young, D.P. Fairlie, J.L. Martin, Structure of West Nile virus NS3 protease: ligand stabilization of the catalytic conformation, J. Mol. Biol. 385 (2009) 1568–1577.
[8] A.E. Aleshin, S.A. Shiryaev, A.Y. Strongin, R.C. Liddington, Structural evidence for regulation and specificity of flaviviral proteases and evolution of the Flaviviridae fold, Protein Sci. 16 (2007) 795–806.
[9] K.J. Chappell, T.A. Nall, M.J. Stoermer, N.-X. Fang, J.D.A. Tyndall, D.P. Fairlie, P.R. Young, Site-directed mutagenesis and kinetic studies of the West nile virus NS3 protease identify key enzyme-substrate interactions, J. Biol. Chem. 280 (2005) 2896–2903.
[10] K.J. Chappell, M.J. Stoermer, D.P. Fairlie, P.R. Young, Insights to substrate binding and processing by West Nile virus NS3 protease through combined modeling, protease mutagenesis, and kinetic studies, J. Biol. Chem. 281 (2006) 38448–38458.
[11] K.J. Chappell, M.J. Stoermer, D.P. Fairlie, P.R. Young, West Nile Virus NS2B/NS3 protease as an antiviral target, Curr. Med. Chem. 15 (2008) 2771–2784.
[12] J. Kouretova, M.Z. Hammamy, A. Epp, K. Hardes, S. Kallis, L. Zhang,

R. Hilgenfeld, R. Bartenschlager, T. Steinmetzer, Effects of NS2B-NS3 protease and furin inhibition on West Nile and Dengue virus replication, J. Enzym. Inhib. Med. Chem. 32 (2017) 712–721.
[13] P.A. Johnston, J. Phillips, T.Y. Shun, S. Shinde, J.S. Lazo, D.M. Huryn, M.C. Myers, B.I. Ratnikov, J.W. Smith, Y. Su, R. Dahl, N.D. Cosford, S.A. Shiryaev, A.Y. Strongin, HTS identifies novel and specific uncompetitive inhibitors of the two-component NS2B-NS3 proteinase of West Nile virus, Assay Drug Dev. Technol. 5 (2007) 737–750.
[14] M. Ezgimen, H. Lai, N.H. Mueller, K. Lee, G. Cuny, D.A. Ostrov, R. Padmanabhan, Characterization of the 8-hydroxyquinoline scaffold for inhibitors of West Nile virus serine protease, Antivir. Res. 94 (2012) 18–24.
[15] H. Lai, G. Sridhar Prasad, R. Padmanabhan, Characterization of 8-hydroxyquinoline derivatives containing aminobenzothiazole as inhibitors of dengue virus type 2 protease in vitro, Antivir. Res. 97 (2013) 74–80.
[16] H.A. Lim, J. Joy, J. Hill, C. San Brian Chia, Novel agmatine and agmatine-like peptidomimetic inhibitors of the West Nile virus NS2B/NS3 serine protease, Eur. J. Med. Chem. 46 (2011) 3130–3134.
[17] S.A. Shiryaev, B.I. Ratnikov, A.V. Chekanov, S. Sikora, D.V. Rozanov, A. Godzik, J. Wang, J.W. Smith, Z. Huang, I. Lindberg, M.A. Samuel, M.S. Diamond, A.Y. Strongin, Cleavage targets and the D-arginine-based inhibitors of the West Nile virus NS3 processing proteinase, Biochem. J. 393 (2006) 503–511.
[18] A. Schuller, Z. Yin, C.S. Brian Chia, D.N. Doan, H.K. Kim, L. Shang, T.P. Loh, J. Hill, S.G. Vasudevan, Tripeptide inhibitors of dengue and West Nile virus NS2B-NS3 protease, Antivir. Res. 92 (2011) 96–101.
[19] C. Nitsche, L. Zhang, L.F. Weigel, J. Schilz, D. Graf, R. Bartenschlager, R. Hilgenfeld, C.D. Klein, Peptide-boronic acid inhibitors of flaviviral proteases: medicinal chemistry and structural biology, J. Med. Chem. 60 (2017) 511–516.
[20] H.A. Lim, M.J.Y. Ang, J. Joy, A. Poulsen, W. Wu, S.C. Ching, J. Hill, C.S.B. Chia, Novel agmatine dipeptide inhibitors against the West Nile virus NS2B/NS3 protease: a P3 and N-cap optimization study, Eur. J. Med. Chem. 62 (2013) 199–205.
[21] A. Bastos Lima, M.A. Behnam, Y. El Sherif, C. Nitsche, S.M. Vechi, C.D. Klein, Dual inhibitors of the dengue and West Nile virus NS2B-NS3 proteases: synthesis, biological evaluation and docking studies of novel peptide-hybrids, Bioorg. Med. Chem. 23 (2015) 5748–5755.
[22] D.T. Scow, G.K. Luttermoser, K.S. Dickerson, Leukotriene inhibitors in the treatment of allergy and asthma, Am. Fam. Physician 75 (2007) 65–70.
[23] E. Gerits, I. Van der Massen, K. Vandamme, K. De Cremer, K. De Brucker, K. Thevissen, B.P.A. Cammue, S. Beullens, M. Fauvart, N. Verstraeten, J. Michiels, M. Roberts, In vitro activity of the antiasthmatic drug zafirlukast against the oral pathogens Porphyromonas gingivalis and Streptococcus mutans, FEMS Microbiol. Lett. 364 (2017).
[24] R.N. Adamek, R.V. Maniquis, S. Khakoo, M.D. Bridges, N.T. Salzameda, A FRET-based assay for the discovery of West Nile Virus NS2B-NS3 protease inhibitors, Bioorg. Med. Chem. Lett 23 (2013) 4848–4850.
[25] S.A. Shiryaev, A.V. Cheltsov, K. Gawlik, B.I. Ratnikov, A.Y. Strongin, Virtual ligand screening of the National Cancer Institute (NCI) compound library leads to the allosteric inhibitory scaffolds of the West Nile Virus NS3 proteinase, Assay Drug Dev. Technol. 9 (2011) 69–78.
[26] S. Sidique, S.A. Shiryaev, B.I. Ratnikov, A. Herath, Y. Su, A.Y. Strongin, N.D.P. Cosford, Structure–activity relationship and improved hydrolytic stability of pyrazole derivatives that are allosteric inhibitors of West Nile Virus NS2B-NS3 proteinase, Bioorg. Med. Chem. Lett 19 (2009) 5773–5777.
[27] V.G. Matassa, T.P. Maduskuie Jr., H.S. Shapiro, B. Hesp, D.W. Snyder, D. Aharony, R.D. Krell, R.A. Keith, Evolution of a series of peptidoleukotriene antagonists: synthesis and structure/activity relationships of 1,3,5-substituted indoles and indazoles, J. Med. Chem. 33 (1990) 1781–1790.
[28] F.J. Brown, Y.K. Yee, L.A. Cronk, K.C. Hebbel, R.D. Krell, D.W. Snyder, Evolution of a series of peptidoleukotriene antagonists: synthesis and structure-activity relationships of 1,6-disubstituted indoles and indazoles, J. Med. Chem. 33 (1990) 1771–1781.
[29] O. Trott, A.J. Olson, AutoDock Vina, Improving the speed and accuracy of docking with a new scoring function, efficient optimization, and multithreading, J. Comput. Chem. 31 (2010) 455–461.
[30] T.A. Nall, K.J. Chappell, M.J. Stoermer, N.-X. Fang, J.D.A. Tyndall, P.R. Young, D.P. Fairlie, Enzymatic characterization and homology model of a catalytically active recombinant West Nile virus NS3 protease, J. Biol. Chem. 279 (2004) 48535–48542.
[31] I. Radichev, S.A. Shiryaev, A.E. Aleshin, B.I. Ratnikov, J.W. Smith, R.C. Liddington, A.Y. Strongin, Structure-based mutagenesis identifies important novel determinants of the NS2B cofactor of the West Nile virus two-component NS2B-NS3 proteinase, J. Gen. Virol. 89 (2008) 636–641.
[32] P.A. Johnston, J. Phillips, T.Y. Shun, S. Shinde, J.S. Lazo, D.M. Huryn, M.C. Myers, B.I. Ratnikov, J.W. Smith, Y. Su, R. Dahl, N.D.P. Cosford, S.A. Shiryaev, A.Y. Strongin, HTS identifies novel and specific uncompetitive inhibitors of the two-component NS2B-NS3 proteinase of West Nile virus, Assay Drug Dev. Technol. 5 (2007) 737–750.
[33] S. Hinsberger, K. Husecken, M. Groh, M. Negri, J. Haupenthal, R.W. Hartmann, Discovery of novel bacterial RNA polymerase inhibitors: pharmacophore-based virtual screening and hit optimization, J. Med. Chem. 56 (2013) 8332–8338.
[34] E.F. Pettersen, T.D. Goddard, C.C. Huang, G.S. Couch, D.M. Greenblatt, E.C. Meng, T.E. Ferrin, UCSF Chimera–a visualization system for exploratory research and analysis, J. Comput. Chem. 25 (2004) 1605–1612.